

Supporting Information

Counterintuitive Catalytic Reactivity of the Aluminum Oxide ‘Passivation’ Shell of Aluminum Nanoparticles Facilitating the Thermal Decomposition of *exo*-Tetrahydrodicyclopentadiene (JP-10)

Souvick Biswas^a, Dababrata Paul^a, Chao He^a, Nureshan Dias^b, Musahid Ahmed^{b*}, Michelle L. Pantoya^{c*}, Ralf I. Kaiser^{a*}

^a Department of Chemistry, University of Hawai’i at Manoa, Honolulu, Hawaii 96822, United States

^b Chemical Sciences Division, Lawrence Berkeley National Laboratory, Berkeley, California 94720, United States

^c Mechanical Engineering Department, Texas Tech University, Lubbock, Texas 79409, United States

* Corresponding author. E-mail: mahmed@lbl.gov

michelle.pantoya@ttu.edu

ralfk@hawaii.edu

S1. Experimental Methods:

S1.1. Synthesis of Aluminum Nanoparticles:

The aluminum nanoparticles (AlNP) were synthesized by heating pure bulk material to elevated temperatures such that liquid atomization formed solid particles. Controlled oxygen concentration is introduced upon droplet formation (and at temperatures less than 400°C) to form a thermodynamically stable amorphous aluminum oxide (Al_2O_3) passivation shell surrounding the metal core. The amorphous shell can range from 3-6 nm thickness (see TEM images, Figure S1). As particle size approaches the nanoscale, alumina becomes an appreciable portion of the total powder concentration. The Al particles were synthesized with a manufacturer reported purity of 87-89 wt.% Al with remaining concentration composed of amorphous alumina. The X-Ray Diffraction (XRD) pattern not only confirms (Figure S2) the purity of Al, but also identify trace concentrations of aluminum oxide hydroxide (AlOOH) in the form of boehmite. The appearance of alumina peak implies that some of the shell has crystalline structure, but it is mainly amorphous. The hydroxylated alumina surface is common with all Al particles, regardless of size. For these NPs, inherently larger concentration of alumina (11-13 wt.% Al_2O_3) also means a higher specific surface area for exposure of the outer particle surface to JP-10 compared with micron-particle Al powders.

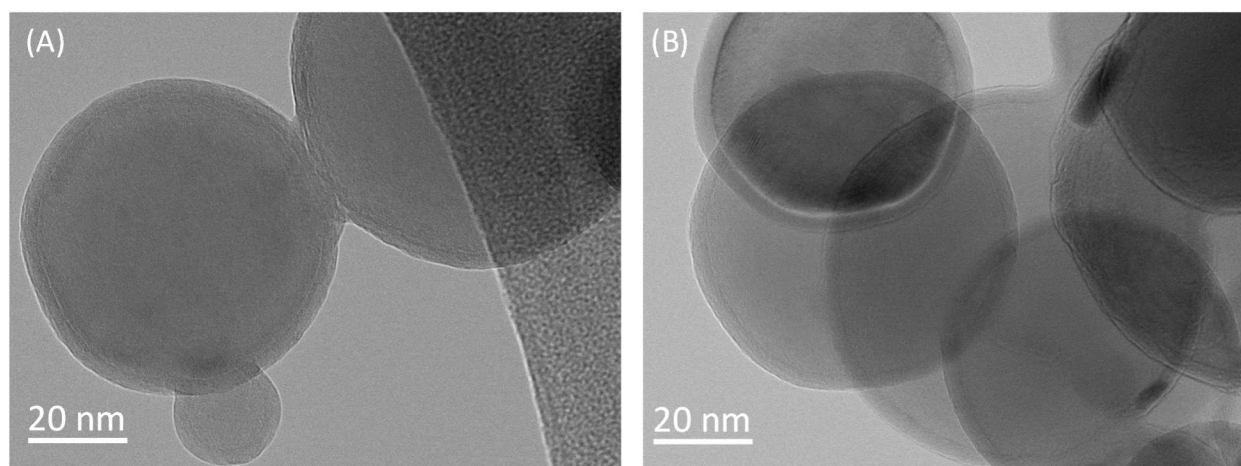


Figure S1: Transmission electron microscopy (TEM) images of alumina (Al_2O_3)-coated aluminum nanoparticles (AlNP).

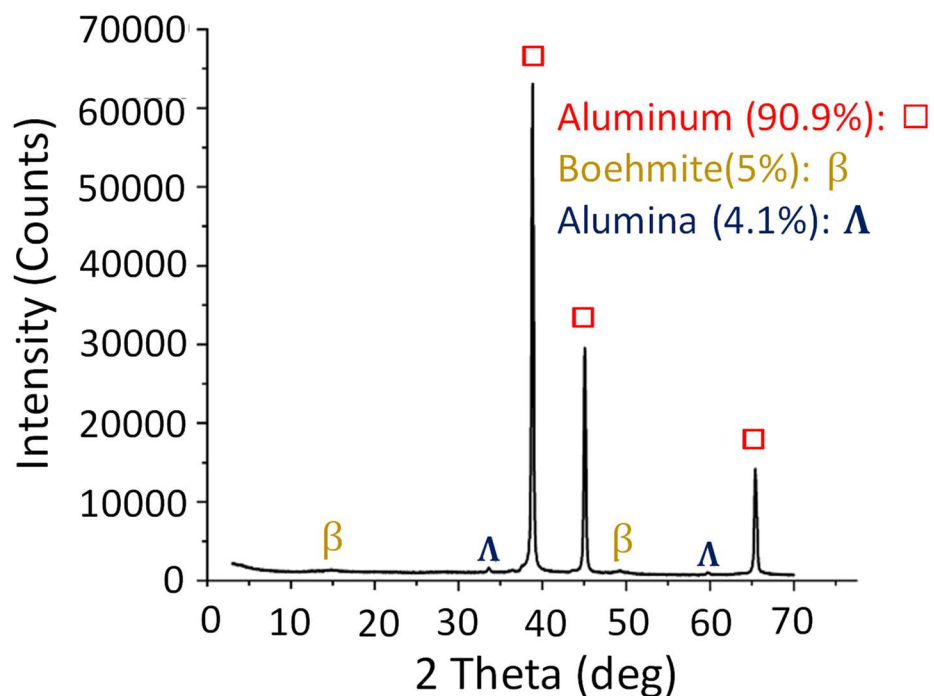


Figure S2: XRD pattern of alumina (Al_2O_3)-coated aluminum nanoparticles (AlNP).

S1.2. High Temperature Chemical Microreactor:

The thermal decomposition experiments were carried out at the Chemical Dynamics Beamline (9.0.2.) installed in Advanced Light Source (ALS) utilizing a high temperature microreactor¹ (Figure S3). Briefly, the high temperature chemical microreactor was a resistively heated silicon carbide (SiC) tube of 20 mm length and 1 mm inner diameter, which was tightly packed with 80 nm sized aluminum nanoparticles (AlNP) about a length of 10 mm inside the SiC tube. Ultimately, the packing is done in such a way so that the interaction and residence time of the fuel with the nanoparticle surface is maximized for optimum reactivity. A gas mixture at a pressure of 500 Torr with JP-10 (*exo*-tetrahydrodicyclopentadiene, $\text{C}_{10}\text{H}_{16}$) (TCI America; 94%) in helium carrier gas (He; Airgas; 99.999%) was prepared by bubbling helium gas through JP-10 kept in a stainless-steel bubbler at 298 K. The gas mixture was introduced into the silicon carbide tube at temperatures up to $1,450 \pm 10$ K as monitored by a type-C thermocouple. After exiting the reactor, the molecular beam, which contained the pyrolysis products, passed a skimmer and entered a detection chamber,

which housed the Wiley-McLaren Reflectron Time-of-Flight Mass Spectrometer (Re-TOF-MS). The products were photoionized in the extraction region of the spectrometer by exploiting quasi-continuous tunable vacuum ultraviolet (VUV) light from the Chemical Dynamics Beamline 9.0.2 of the Advanced Light Source and detected with a microchannel plate (MCP) detector.

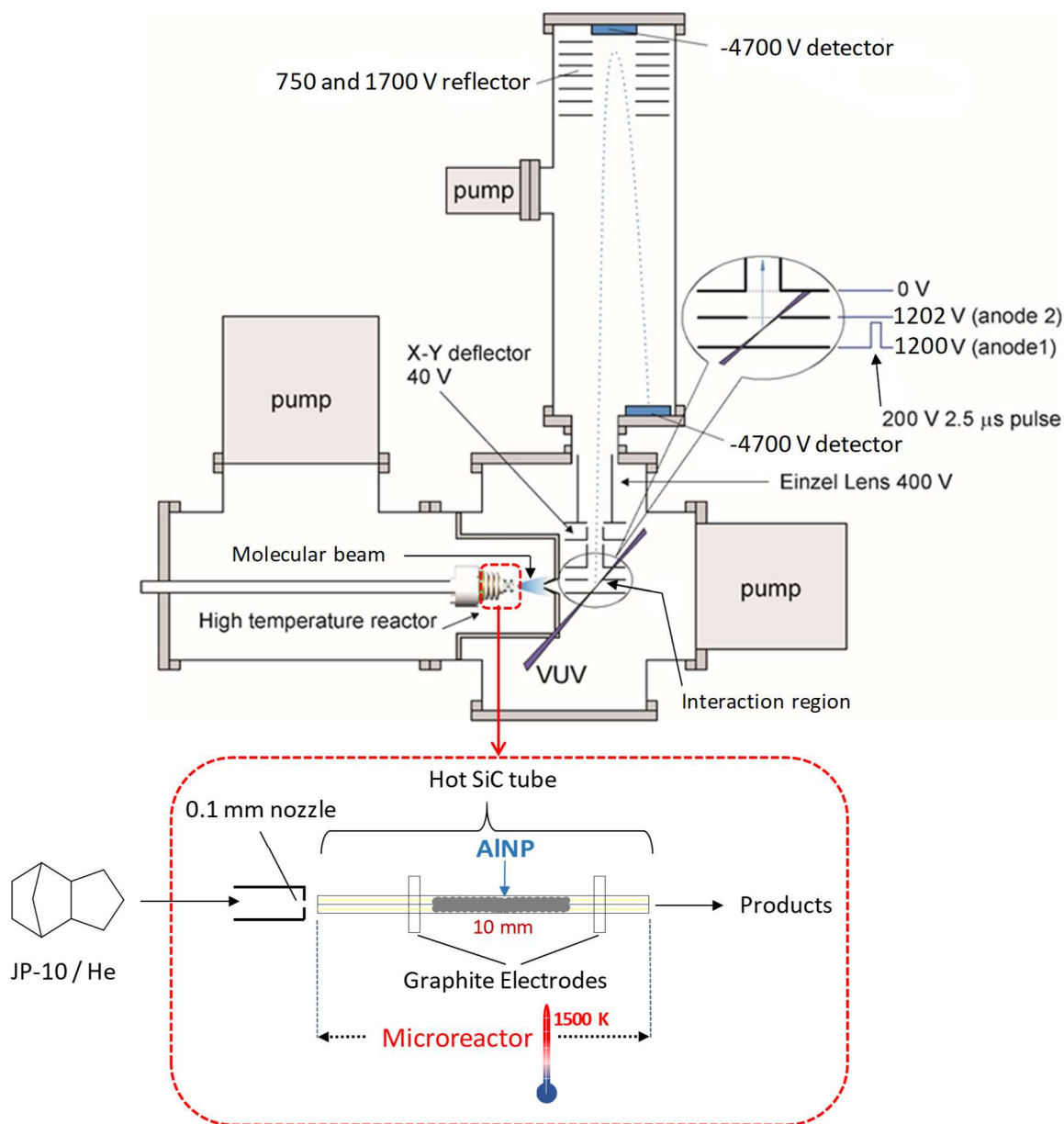
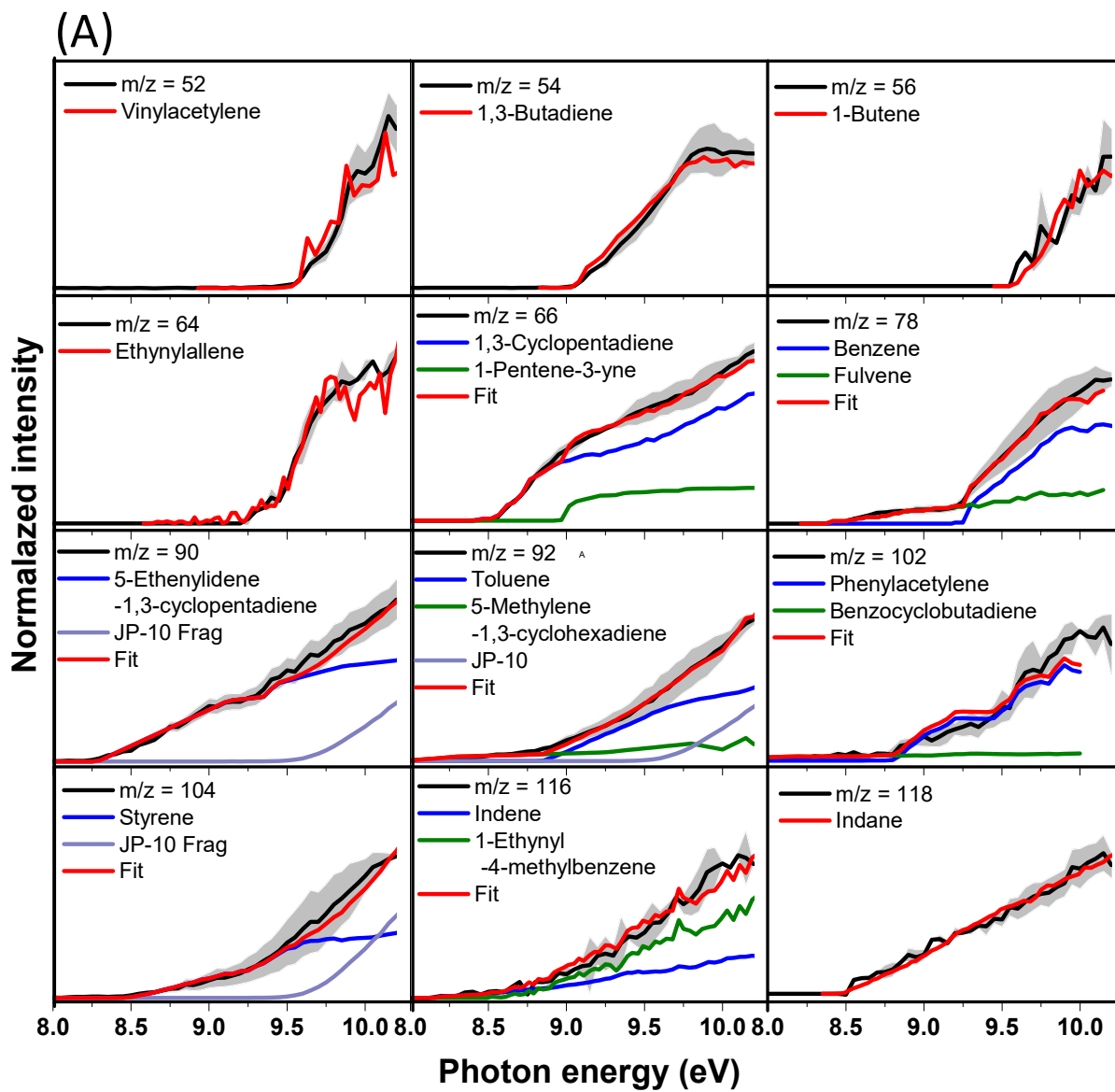


Figure S3: Schematic of the experimental setup including high temperature microreactor and Reflectron Time-of-Flight Mass Spectrometer (Re-TOF-MS).

Here, mass spectra were recorded in 0.05 eV intervals from 8.00 eV to 11.50 eV. A set of additional mass spectra was also measured at 15.4 eV to determine hydrogen and methane yields having ionization energies of 15.4 eV and 12.6 eV, respectively, which cannot be ionized below 11.5 eV. The photoionization efficiency (PIE) curves, which report the intensity of a single mass-to-charge ratio (m/z) versus the photon energy, were extracted by integrating the signal collected at a specific m/z selected for the species of interest over the range of photon energies in 0.05 eV increments and normalized to the incident photon flux. The PIE curves were then fit with a linear combination of known PIE curves to isomer-selectively identify the products. The residence time of JP-10 in the reactor tube (20 mm) under our experimental conditions are tens of ms. This would result in typically three to four (1,500 K) collisions of a JP-10 molecule with the helium atoms in the reactor at 500 Torr. However, as the pressure drops from 500 Torr to a few Torr at the exit of the reactor, the actual number of collisions is about one on average.



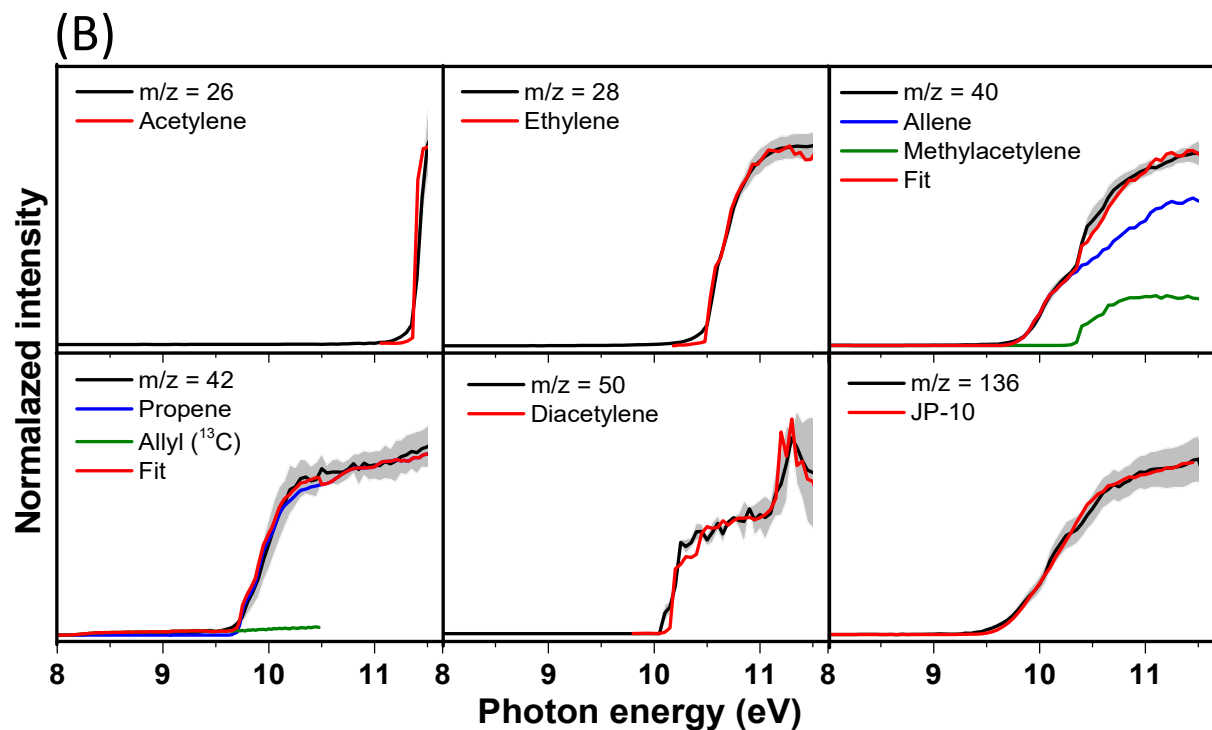


Figure S4: Experimental photoionization efficiency curves (PIE, black traces) for the hydrocarbon products formed upon thermal decomposition of JP-10 on AlNP recorded in the range of (A) 8.0 - 10.2 eV and (B) 8.0 - 11.5 eV. The experimental errors are indicated by gray area, the reference PIE curves and the overall fitted curve (red trace) in case of multiple isomeric contribution are also presented. JP-10 fragment implies the photolysis fragment of JP-10 generated upon dissociative photoionization.

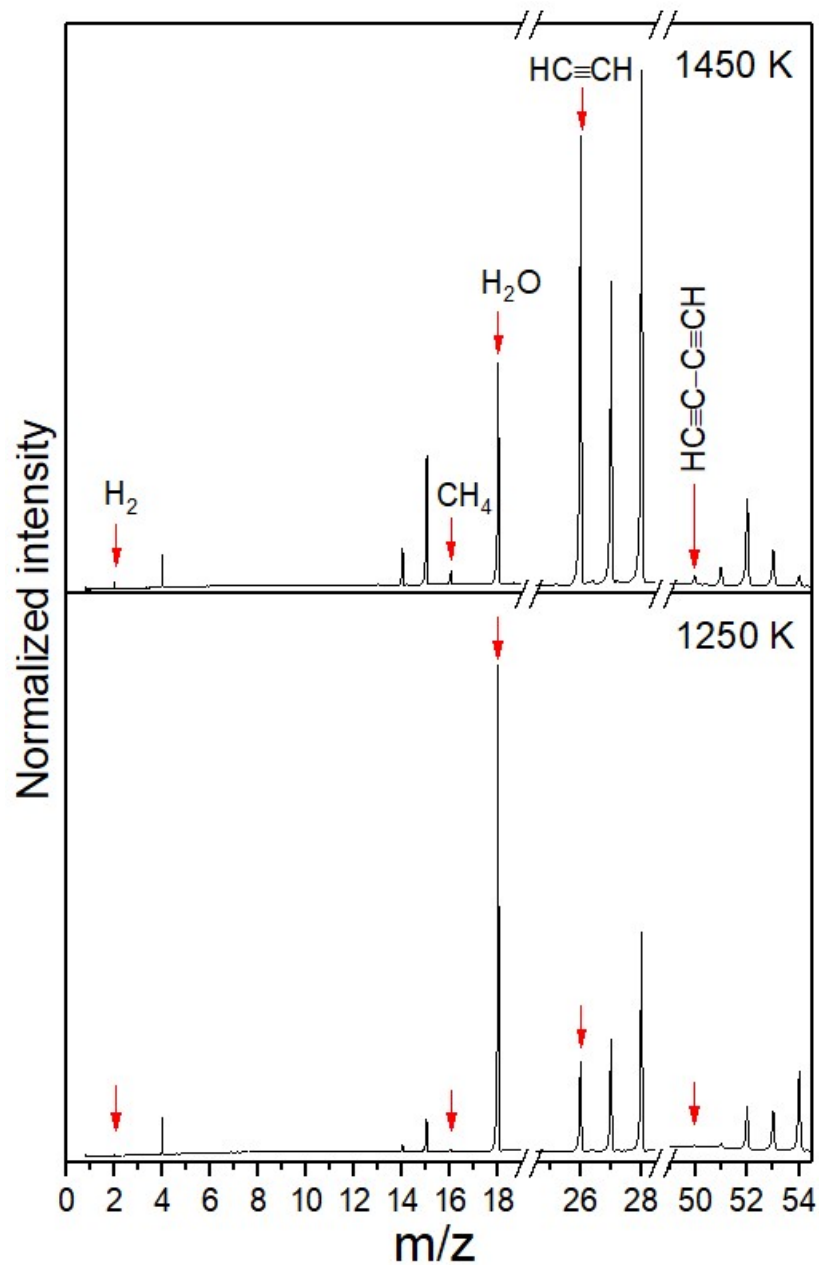
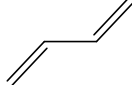
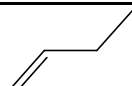
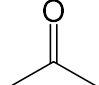
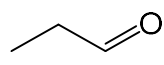
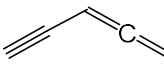
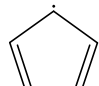

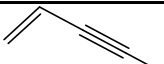
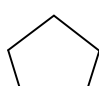
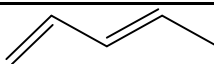
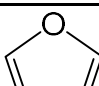

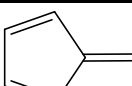
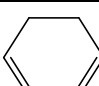
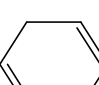
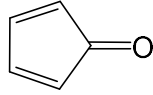
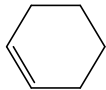
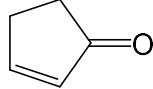
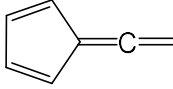
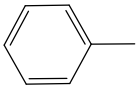
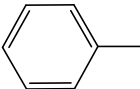
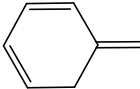
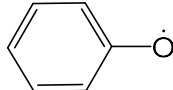
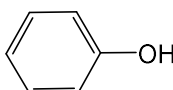
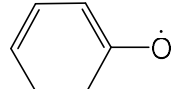
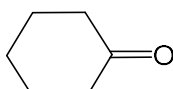
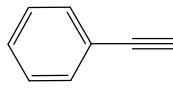
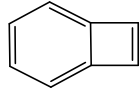


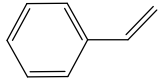
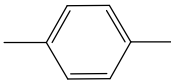
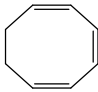
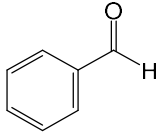
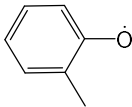
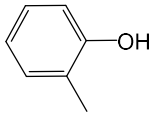
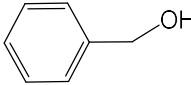
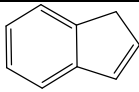
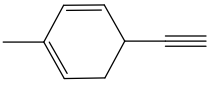
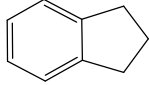
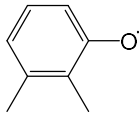
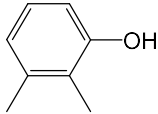
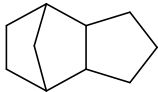
Figure S5: Mass spectra recorded at a photon energy of 15.4 eV to show a few relevant thermally decomposed products [hydrogen (H_2), methane (CH_4), water (H_2O), acetylene (C_2H_2) and diacetylene (C_4H_2)] of JP-10 through aluminum nanoparticles (AlNP) at 1,250 and 1,450 K.

Table S1: Compilation of the products with corresponding ionization energies observed in the thermal decomposition of JP-10 on AlNP.²⁻³

Mass	Molecular formula	Name	Structure	Ionization energy (eV)
2	H ₂	Hydrogen	H-H	15.4
15	CH ₃	Methyl radical	$\cdot\text{CH}_3$	9.8
16	CH ₄	Methane	CH ₄	12.6
18	H ₂ O	Water		12.6
26	C ₂ H ₂	Acetylene	HC≡CH	11.4
27	C ₂ H ₃	Vinyl radical	CH ₂ =CH \cdot	8.3
28	C ₂ H ₄	Ethylene	CH ₂ =CH ₂	10.5
29	C ₂ H ₅	Ethyl radical	CH ₃ -CH ₂ \cdot	8.1
	CHO	Formyl radical		8.1
39	C ₃ H ₃	Propargyl radical		8.7
40	C ₃ H ₄	Allene		9.7
		Methylacetylene		10.4
41	C ₃ H ₅	Allyl radical		8.1
	HC ₂ O	Ethynyloxy radical		9.5
42	C ₃ H ₆	Propene		9.7
43	AlO	Aluminum monoxide	$\cdot\text{Al}=\text{O}$	9.6
50	C ₄ H ₂	Diacetylene		10.1
52	C ₄ H ₄	Vinylacetylene		9.6

54	C_4H_6	1,3-Butadiene		9.1
56	C_4H_8	1-Butene		9.6
58	C_3H_6O	Acetone		9.7
		Propanal		9.9
64	C_5H_4	Ethynylallene		9.2
65	C_5H_5	Cyclopentadienyl radical		8.4
66	C_5H_6	1,3-Cyclopentadiene		8.5
		1-Penten-3-yne		9.0
68	C_5H_8	Cyclopentene		9.2
		1,3-Pentadiene		8.6
	C_4H_4O	Furan		8.9
78	C_6H_6	Benzene		9.2
		Fulvene		8.4
80	C_6H_8	1,3-Cyclohexadiene		8.3
		1,4-Cyclohexadiene		8.8

	C_5H_4O	2,4-Cyclopentadiene-1-one		9.4
82	C_6H_{10}	Cyclohexene		8.9
	C_5H_6O	2-Cyclopenten-1-one		9.4
90	C_7H_6	5-Ethenylidene-1,3-cyclopentadiene		8.3
91	C_7H_7	Benzyl radical		7.2
92	C_7H_8	Toluene		8.8
		5-Methylene-1,3-cyclohexadiene		7.9
93	C_6H_5O	Phenoxy radical		8.6
94	C_6H_6O	Phenol		8.5
95	C_6H_7O	1,3-Cyclohexadienyloxy radical		9.0
96	C_6H_8O	2-Cyclohexen-1-one		9.2
102	C_8H_6	Phenylacetylene		8.8
		Benzocyclobutadiene		7.5

104	C_8H_8	Styrene		8.4
106	C_8H_{10}	p-Xylene		8.5
		1,3,5-Cyclooctatriene		7.9
	C_7H_6O	Benzaldehyde		9.5
107	C_7H_7O	Methylphenoxy radical		8.3
108	C_7H_8O	Cresols		8.3
		Benzyl alcohol		9.0
116	C_9H_8	Indene		8.3
		1-Ethynyl-4-methylbenzene		8.5
118	C_9H_{10}	Indane		8.5
121	C_8H_9O	Dimethylphenoxy radical		8.3
122	$C_8H_{10}O$	Dimethylphenol		8.2
136	$C_{10}H_{16}$	JP-10		9.5

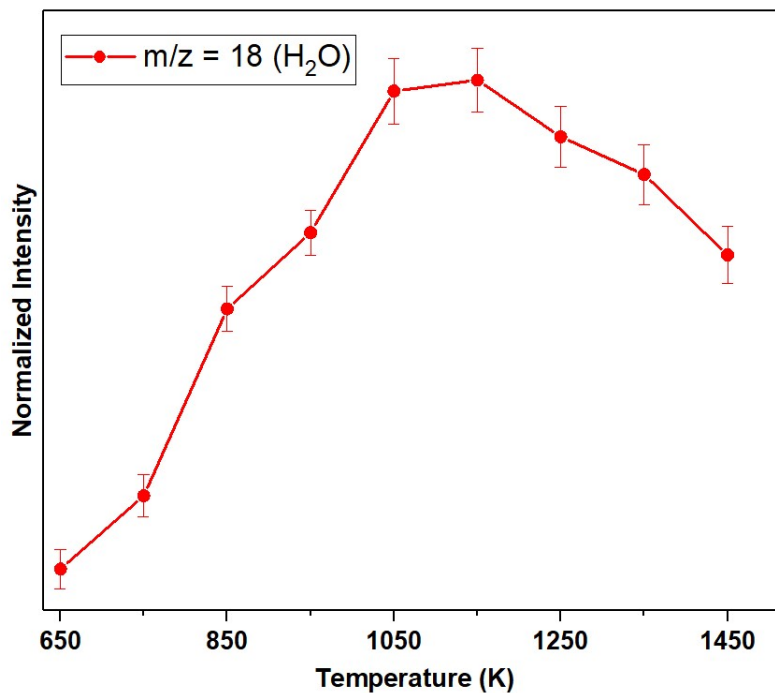


Figure S6: Temperature dependant abundances of water (H_2O) due to thermal decomposition of JP-10 by AlNP.

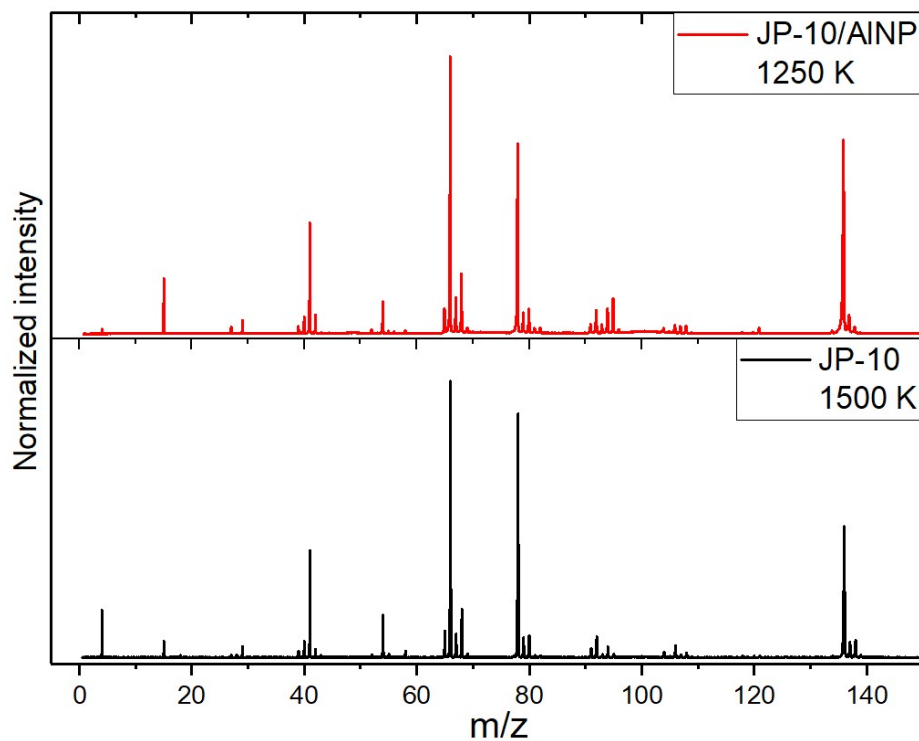


Figure S7: Comparison of the mass spectra obtained upon thermal decomposition of JP-10; without any additive (black trace) at 1,500 K¹ and with AlNP (red trace) at 1,250 K.

S2. Quantification of Temperature Dependent Oxygen Uptake Coefficient from Alumina Oxide Shell:

Estimation of the total oxygen content in the alumina oxide shell material is as follows.

Total volume of aluminum nanoparticles (AlNP) incorporated inside the silicon carbide tube

$$= 3.14 \times (0.05)^2 \times 1 \text{ cm}^3 = 0.00785 \text{ cm}^3$$

Total mass of aluminum nanoparticles (AlNP) incorporated inside the silicon carbide tube

$$= 0.00785 \text{ cm}^3 \times 2.7 \text{ g cm}^{-3} = 0.021195 \text{ g}$$

Effective mass of the alumina oxide shell material of aluminum nanoparticles (AlNP) assuming 15 wt.% composition = $0.021195 \times 0.15 \text{ g} = 0.00317925 \text{ g}$

Number of moles of available oxygen atom in the alumina oxide shell material

$$= (0.00317925 \text{ g} / 101.96 \text{ g mol}^{-1}) \times 3 = 9.35 \times 10^{-5}$$

The number of moles for JP-10 vapor introduced in the molecular beam = 1.97×10^{-4}

The number of moles for the total oxygenated products have been calculated from the branching ratio (Figure 4) of respective products and calculation of the temperature dependent oxygen uptake coefficients from aluminum oxide shell to oxygenated molecules and radicals have been presented in Table S2.

Table S2: Temperature dependent oxygen uptake coefficients from aluminum oxide shell to oxygenated molecules and radicals.

Temperature (K)	Total moles of oxygenated products	Oxygen uptake coefficients
650	9.9×10^{-6}	0.11 ± 0.04
850	3.1×10^{-5}	0.33 ± 0.05
1050	4.3×10^{-5}	0.44 ± 0.09
1250	2.9×10^{-5}	0.31 ± 0.10
1450	1.1×10^{-5}	0.10 ± 0.07

References:

1. Zhao, L.; Yang, T.; Kaiser, R. I.; Troy, T. P.; Xu, B.; Ahmed, M.; Alarcon, J.; Belisario-Lara, D.; Mebel, A. M.; Zhang, Y.; Cao, C.; Zou, J., A Vacuum Ultraviolet Photoionization Study on High-Temperature Decomposition of JP-10 (exo-Tetrahydrodicyclopentadiene). *Phys. Chem. Chem. Phys.* **2017**, *19*, 15780-15807.
2. Linstrom, P.J.; Mallard, W.G. *NIST Chemistry WebBook, NIST Standard Reference Database Number 69*.
3. Photonization Cross Section Database (Version 2.0), National Synchrotron Radiation Laboratory, Hefei, China, 2017.